journal

J. Am. Ceram. Soc., 77 [1] 137–42 (1994)

Fatigue Crack Growth of Silicon Nitride at 1400°C: A Novel Fatigue-Induced Crack-Tip Bridging Phenomenon

Shih-Yu Liu,* I-Wei Chen,* and Tseng-Ying Tien*

Department of Materials Science and Engineering, The University of Michigan, Ann Arbor, Michigan 48109-2136

A high-strength Si_3N_4 with elongated β-Si_3N_4 and equiaxed α′-sialon was tested in cyclic and static fatigue at 1400°C. At low stress intensity factors and high frequencies, the pullout process of the elongated grains was enhanced, which suppressed the crack growth. This provides a possible explanation for the increased lifetime under cyclic loading conditions reported for ceramics by several investigators. While crack-healing by high-temperature annealing was found to greatly reduce the subsequent static fatigue crack growth rate, it had only a modest effect on cyclic fatigue and none at high frequencies.

I. Introduction

THE common observations for mechanical fatigue of structural ceramics at room temperature are a shorter lifetime and a higher crack growth rate under cyclic loading (i.e., cyclic fatigue) compared to static loading (i.e., static fatigue).[1–22] This is further supported by the observation that the fatigue lifetime is more cycle-dependent than time-dependent. On the other hand, a number of investigators have reported the opposite phenomenon of a longer cyclic fatigue lifetime when the fatigue tests were conducted at elevated temperatures.[23–31] (This is despite the early report on pure Al_2O_3 which showed little difference in static and cyclic fatigue crack growth rates.[32–34]) An opposite frequency effect, i.e., a greater cycles to failure at a higher frequency,[27] was also noted. Clearly, qualitatively different damage mechanisms must operate in different temperature regimes.

One reason for a longer cyclic fatigue life lies in the smaller fraction of time spent under high stress during cycling. This difference can be accounted for by defining an effective stress (intensity factor) or effective time if damage assumed is to accumulate in the same way as in static fatigue at the same stress (intensity factor) level. Several studies have shown, however, that even with such an adjustment, the cyclic fatigue lifetime was systematically longer than the static one. Some direct fatigue crack growth measurements at elevated temperatures for a commercial Al_2O_3 and an Al_2O_3–SiC composite also seem to support the same notion of fatigue retardation.[28–31] No mechanistic explanation, to our knowledge, has been offered to rationalize these observations.

Si_3N_4 is an important structural ceramic with current and potential applications at elevated temperatures.[35] To our best knowledge, direct measurement of fatigue crack growth rates has not been made for this class of material. In this study, we will report the crack growth behavior in a hot-pressed Si_3N_4 which has a relatively high strength at elevated temperatures (750 MPa at 1400°C).[35] A multiple controlled-flaw technique was used allowing efficient data acquisition without *in situ* crack length monitoring. This first report will focus on the results obtained at 1400°C which revealed some novel frequency effects and crack-tip phenomena. These observations have provided new insight to the cause of fatigue retardation at elevated temperatures.

II. Experimental Procedure

(1) Material

The silicon nitride studied was a two-phase material containing α′-sialon (30 vol%) and β-Si_3N_4 (70 vol%). The composition chosen is along the Si_3N_4–Y_2O_3:9AlN composition line and lies on the so-called α′-sialon phase. Details of material design, processing conditions, and preliminary mechanical properties of this series of materials will be published elsewhere.[35] The material studied was hot-pressed at 1780°C in N_2 for 1 h to reach full density. Scanning electron microscopy examination revealed a microstructure containing many elongated β-Si_3N_4 grains, as evident from Fig. 1. X-ray diffraction and transmission electron microscopy further verified the existence of β-Si_3N_4 and α′-sialon phases, the latter being interdispersed in the form of small equiaxed particles between elongated β-Si_3N_4 grains. This duplex microstructure results in a very low Al and Y content in the grain boundary and hence minimizes the adverse impact of low-viscosity glassy phase. Excellent flexural strength has been measured in four-point bending in air at room temperature (1050 MPa) and elevated temperature (750 MPa at 1400°C).[35]

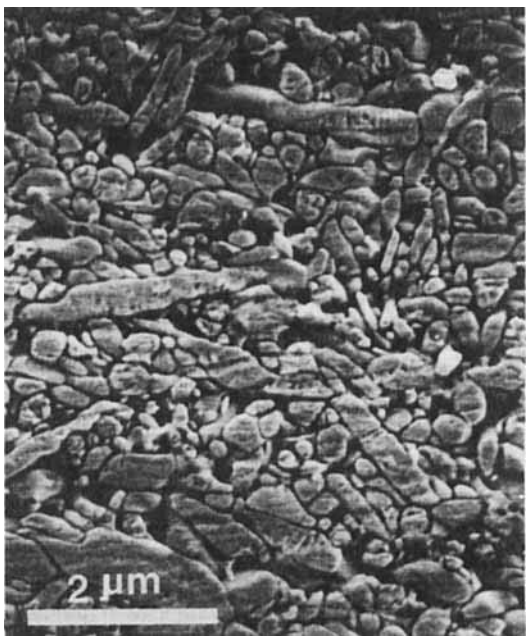

Fig. 1. Microstructure of hot-pressed Si_3N_4.

D. Wilkinson—contributing editor

Manuscript No. 194882. Received February 8, 1993; approved August 20, 1993.
Supported by the U.S. Air Force under Grant No. AFOSR-91-0094.
*Member, American Ceramic Society.

(2) Specimens

Bend bars with dimensions of 17 mm × 3 mm × 1.2 mm were obtained from the hot-pressed material. The long axis of the specimen lies on the hot-pressing plane and the tensile surface lies normal to the hot-pressing plane. The surface of the specimen was finely ground along the long axis, then polished using a 6-μm diamond paste to obtain a good finish. A series of Vickers indents was placed on the tensile surface at a load of 12 kg. These indents were 0.5 mm apart and carefully aligned so that corner cracks emanating from the indents were all parallel or perpendicular to the long axis of the specimen. To remove the residual stress around the indent before fatigue testing, two kinds of heat treatment were performed. In the first treatment, specimens were held at 1400°C for 1 h under a flexural load of 50 N. Depending on the local flexural stress, a typical crack extension of 10 to 40 μm was obtained after this treatment. In the second treatment, specimens were held at 1400°C for 1 h without a load. No change in crack length was found after this treatment.

(3) Fatigue Testing

A modified four-point bending configuration with an inner span of 1.25 mm and an outer span of 13 mm was used in this study. It provides a long outer span where the (linear) stress distribution, regardless of the contact conditions at the two loading points, can be accurately determined. At the same time, there is a short inner span within which the stress is essentially constant but could have some variation due to uneven loads at the inner contacts. Usually, 3 indents were placed within the inner span and 10 other indents on each end outside. The adoption of this configuration facilitated data acquisition over a relatively broad range of crack extension force from one specimen. When the specimen eventually failed from one of the cracks in the inner span, the two remaining cracks could be used for critical crack length measurement and microscopy since they had experienced essentially the same load history and were near critical length.

Cyclic bending fatigue tests were conducted using a commercial servohydraulic machine (Model 810, MTS Test Systems Inc., Minneapolis, MN) operated under load control, with a sinusoidal wave form. The specimen was first heated to 1400°C at a rate of 60°C/min. The load was then slowly applied at a ramp rate of 5 N/s until the maximum stress level was reached. The maximum nominal stress was 172 MPa and the R-ratio (minimum stress/maximum stress) was 0.1. Three frequencies (0.1, 1, and 5 Hz) were used to evaluate the frequency effect. For comparison, static fatigue tests at the same temperature and held at the same maximum stress were also conducted. All fatigue tests were terminated after 20 h unless failure occurred sooner. The load was removed during cooling, which was estimated to occur at a rate of 75°C/min. Crack length was measured after testing using an optical microscope.

(4) Data Processing

The applied stress intensity factor at the tip of a semielliptical surface crack subject to pure bending was calculated from the finite element analysis of Newman *et al.*[36] The aspect ratio, a/b, for the semielliptical crack was approximated by using an empirical equation recommended by ASTM E 740:[37]

$$\frac{a}{b} = \frac{a}{t} + 1 \tag{1}$$

where a and b are the half crack length of the major and minor axis, respectively, and t is the specimen thickness. Since it was assumed that most of the residual stress due to indentation had been removed during the heat treatment prior to fatigue testing, the applied stress intensity factor was taken as the only driving force for crack extension.

Under such a driving force, the slow crack growth rate may be assumed to follow a power law relation:

$$\frac{da}{dt} = AK^n \tag{2}$$

where A and n are constants, and K is the stress intensity factor at the crack tip. For static fatigue, K is constant until crack extension. For cyclic fatigue K varies from a minimum (K_{min}) to a maximum (K_{max}) during each cycle. For the latter case, two expressions have been used to compare the crack growth rate. The first is identical to Eq. (2), but with K replaced by K_{max} during a cycle; such an expression is adequate for the present study in which the R-ratio was held at 0.1. In the second expression, the same power law relation is used, but allowing the stress intensity factors to vary with time. The following expression after integration over time is arrived at:

$$\frac{da}{dt} = AK_{eff}^n \tag{3}$$

In the above, K_{eff} may be regarded as the effective stress intensity factor in static fatigue that will result in the same amount of crack growth over time as in cyclic fatigue. For sinusoidal loading profile, simple integration shows

$$K_{eff} = K_{max}\left\langle\left[\frac{1+R}{2} + \frac{1-R}{2}\sin(2\pi\omega t)\right]^n\right\rangle^{1/n}$$

$$= K_{max}F(n,R) \tag{4}$$

In the above equation, ω is frequency, and $F(n,R)$ may be viewed as a correction factor for converting K_{max} to K_{eff}. This correction factor is plotted in Fig. 2. It can be seen that the effective stress intensity factor, which is independent of frequency ω, decreases drastically as the exponent, n, and stress ratio, R, decrease.

The constants A and n can best be obtained by least-squares fitting of the measured crack growth data. Although *in situ* crack growth rate measurements were not performed, there were sufficient crack length data from each test for such a fit. (For each crack, the initial length and the final length were recorded. Since these cracks were of various initial lengths and subject to various stresses, they grew to various lengths during testing. Typically there were about 10 to 15 data of significant crack extension to best-fit two unknowns for each test using regression analysis. For this reason, this form of data analysis is referred to in the following as the "regression method".) Once these constants have been determined, the crack growth rate in static fatigue and cyclic fatigue under various loading conditions can be compared on the basis of K_{max} or K_{eff}. A comparison on the basis of K_{max} allows us to assess the relative severity of creep and cyclic damage. Alternatively, a comparison on the

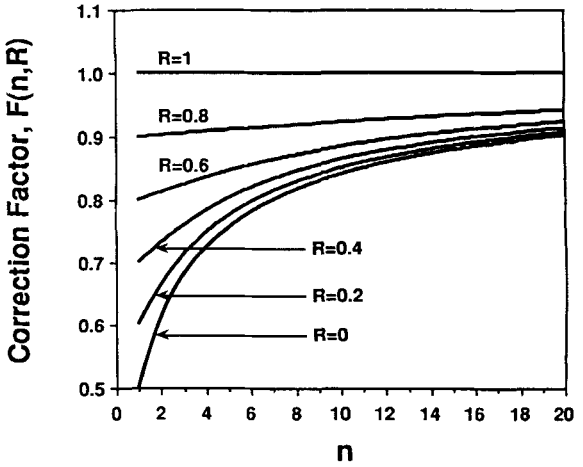

Fig. 2. Correction factor $F(K_{eff}/K_{max})$ as a function of R and n.

basis of K_{eff} highlights the additional cyclic loading effect by relating to the slow crack growth equation.

To compare with the regression method described above, the conventional "average" method was also performed. In the latter case, the average crack growth rate for each indent was obtained by dividing the total crack extension by test duration, and the average stress intensity factor was the mean value of the maximum stress intensity factors associated with the initial and final crack lengths.

III. Results and Discussion

(1) Frequency Effect

Table I summarizes the test results for specimens heat-treated at 1400°C under a preload of 50 N. The A, n, and $F(n,R)$ values obtained from both regression and average methods are shown for each test condition. The n values obtained from the average method are only slightly smaller, indicating that the crack extension curves are essentially straight lines with a slightly concave upward curvature. The comparison is shown graphically in Fig. 3. In Fig. 3(a), two data points corresponding to the initial and final crack growth rates inferred from the regression method are drawn for each crack, while in Fig. 3(b), each datum represents the average crack growth rate for each crack. Despite the larger scattering of the data analyzed by the average method (Fig. 3(b)), the trend and the magnitude of the data are essentially the same as those from the regression method (Fig. 3(a)). In view of the similarity, only data processed by regression are presented in the following discussion.

Several interesting features in Fig. 3 which compare crack growth rates at the same K_{max} under different loading conditions are worthy of note. First, it is apparent that at 1400°C the crack growth rates under cyclic loading conditions are always less than those under static loading conditions. Second, the crack growth retardation due to cyclic loading is much more pronounced at higher frequency and lower stress intensity. Third, cyclic fatigue at higher frequency has a higher K_{max} sensitivity, i.e., a larger n exponent. Fourth, the value of n exponent is relatively small, ranging from 4 to 9. These features are unique to high-temperature fatigue. (The opposite trend is typically seen for ceramics at low temperature; i.e., the crack growth rate is higher in cyclic fatigue, the enhancement is more pronounced at higher frequency and lower stress intensity, and cyclic fatigue has a lower stress intensity exponent which is nevertheless very large in magnitude, typically above 20.) The crack growth rate is also plotted against the effective stress intensity factor (K_{eff}) as shown in Fig. 4. In such a plot, the effect of unloading from K_{max} has been taken into account explicitly. Note that at 0.1 Hz, the crack growth rate is reduced to the same as in static loading once the unloading effect is considered. Thus, at least at low frequencies, the crack growth mechanism in static and cyclic loading seems to be the same. At higher frequencies, however, a genuine retardation due to cyclic loading becomes apparent. This retardation is more pronounced at higher frequency and lower stress intensity factor as evident from the n exponent which changes from 4.4 to 8.4. Obviously, a different damage/crack growth mechanism must be involved at higher frequencies.

The slower crack growth rates at higher frequency arising from the unloading portion of the cycle may be due to either

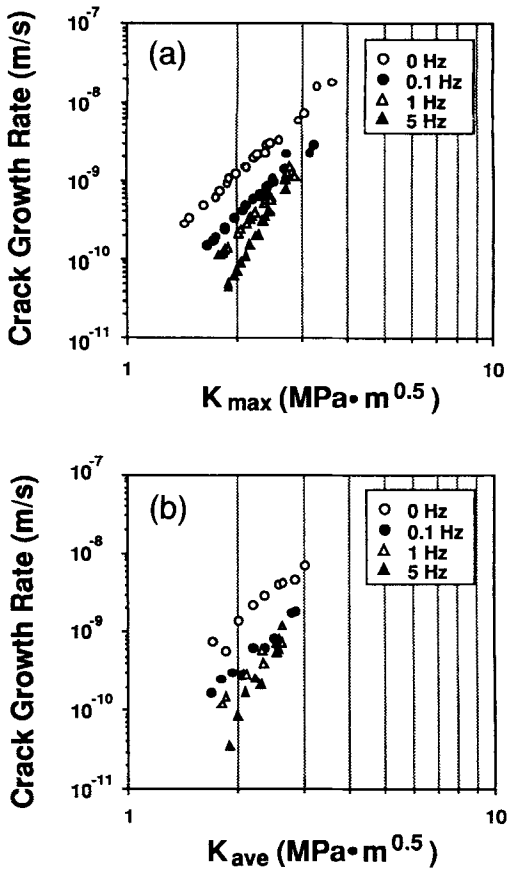

Fig. 3. Crack growth rates against maximum stress intensity factors (a) by regression method and (b) by average method.

enhanced pullout of elongated grains or formation of load-bearing contacts, as schematically shown in Fig. 5. In either case, the effective stress intensity at the crack tip is somewhat reduced. In the following, we will discuss the relevance of these two mechanisms to our observations of fatigue retardation.

(a) Crack Face Contact—This can be caused by deformation irreversibility during unloading (Fig. 5(b)).[38] Below a certain load, the crack tip stress intensity factor is sufficiently reduced by such contacts, so that the static fatigue effect is largely mitigated (Fig. 5(c)). Since creep and grain boundary sliding are more active at high temperature, displacement irreversibility is enhanced, which in turn causes significant retardation of crack growth in cyclic loading. It is known that, at low temperature, crack shielding by closure is most affected by the R-ratio but not frequency. This R-ratio dependence is likely to prevail at high temperature although it has not been investigated. A frequency effect, however, is also likely to arise at high temperature in view of the strain rate dependence of grain boundary sliding and creep.[39] Since a lower frequency should promote more creep and grain boundary sliding, it favors more closure and retardation. This is contrary to our observations.

(b) Grain Pullout—This can be caused by repeated sliding between grains which weakens the grain/grain interface. (In

Table I. Fatigue Data at Different Frequencies

Cyclic frequency (Hz)	n		A		Correction factor, $F(n,R)$		Test duration (h)
	Regression	Average	Regression	Average	Regression	Average	
5	8.39	8.18	2.10×10^{-13}	2.76×10^{-13}	0.8279	0.8279	20
1	5.45	5.16	4.53×10^{-12}	5.96×10^{-12}	0.7715	0.7715	20
0.1	4.52	4.25	1.52×10^{-11}	1.80×10^{-11}	0.7471	0.7471	20
Static	4.42	4.16	5.63×10^{-11}	7.09×10^{-11}	1	1	8.8

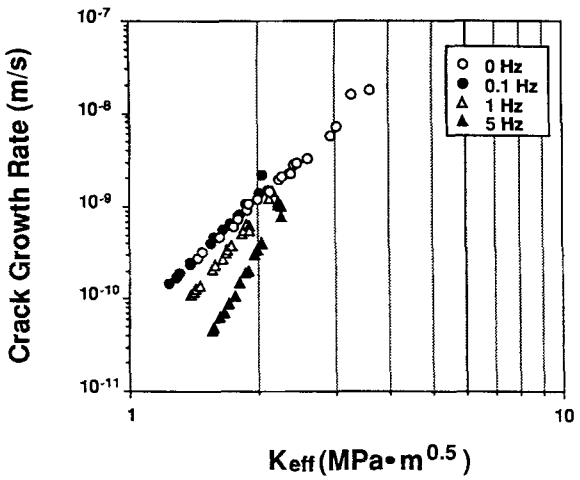

Fig. 4. Crack growth rates in static fatigue and cyclic fatigue at different frequencies against the effective stress intensity factor.

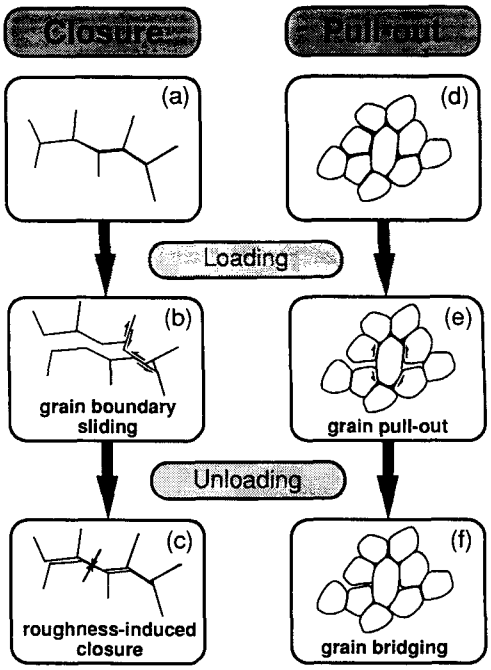

Fig. 5. Schematics of possible fatigue crack growth retardation mechanisms at high temperatures.

mechanism (a), no degradation of grain/grain interface by sliding is assumed.) At higher temperature, traction for grain boundary sliding is sufficiently reduced to allow grain pullout without grain fracture (Figs. 6(e) and (f)). Cycling at high frequency will accumulate more damage to weaken the interface even more to facilitate this process. This is in agreement with our observation. At higher stress intensity factors, the chance of breaking grains at the crack tip before their pullout is substantially increased. Therefore, this shielding mechanism is lost. The crack growth rate then increases to approach that in static fatigue. This is also in agreement with our observation.

The physical evidence of the pullout mechanism is relatively difficult to obtain for two reasons. First, it was found that numerous needlelike small grains nucleated and grew on the tensile surface of the specimen after long-term exposure to the flowing nitrogen atmosphere at high temperatures. This renders the disclosure of fine details of the crack tip difficult. Second, the remains of broken bridges may be damaged by repeated abrasion of crack faces during cycling. Hence, the difference in crack morphology between cyclic and static fatigue is not always apparent. Despite these problems, some features that support the above mechanism have been found on the tensile surface near the crack tip. One example from a specimen cycled at a relatively high frequency and relatively low stress intensity factor (5 Hz and 2.3 MPa·m$^{1/2}$) is shown in Fig. 6. At the crack tip, an elongated grain that has been pulled out for about 2 μm and damaged by a tiny crack (indicated by arrows) can be seen in Fig. 6(a). Further back in the crack wake, several broken grains with a similar pullout distance can also be seen in Fig. 6(b). Such pulled-out grains with a long pullout distance were rarely observed in specimens tested in static fatigue.

Finally, the onset of the pullout mechanism may introduce a rising crack wake shielding in the initial stage of crack extension. During this transient period, the power law growth expressions, Eqs. (2) and (3), and their counterpart in cyclic fatigue,

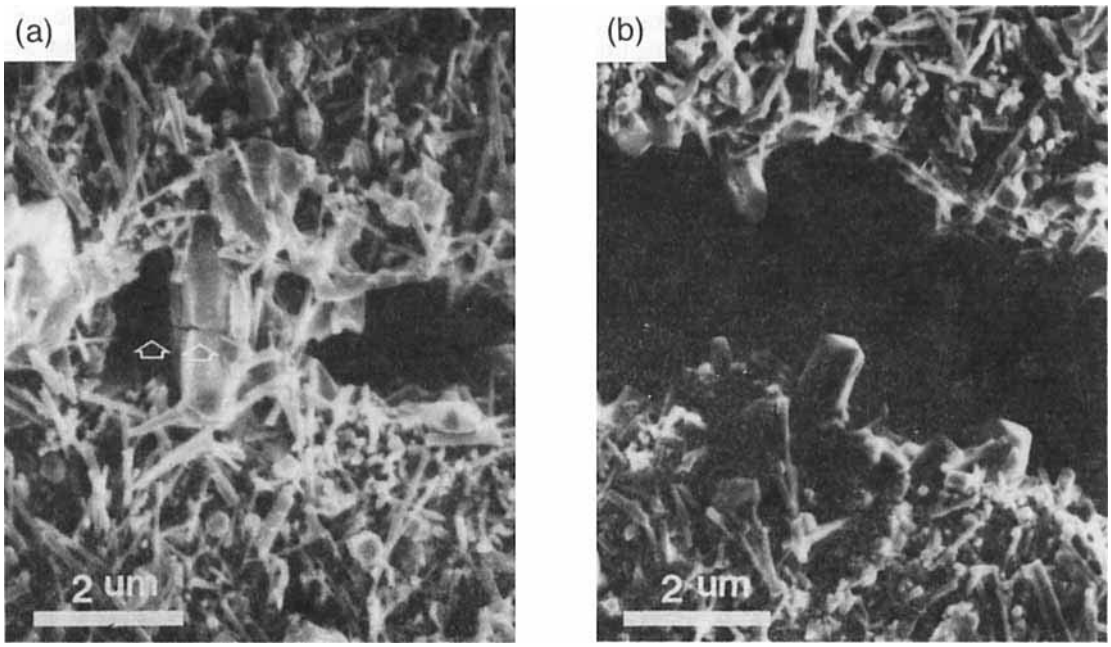

Fig. 6. SEM micrographs of an indentation crack fatigued at 5 Hz and K_{max} = 2.3 MPa·m$^{0.5}$: (a) near the crack tip and (b) in the crack wake.

are not applicable unless the shielding stress intensity factor is explicitly incorporated in the expressions. A short-crack behavior is thus anticipated. This aspect is under investigation elsewhere.[40] For the present set of experimental conditions, however, the crack extension curves are believed to be nearly straight lines. Thus any short-crack behavior, if present, is probably very short-lived and not expected to significantly compromise the validity of the data analysis used here.

(2) Annealing Effect

The stress applied in the 1400°C heat treatment prior to fatigue testing was found to have a significant effect on the subsequent crack growth. This is illustrated by the data in Fig. 7. Here we compare crack growth data from specimens heat-treated with a preload (represented by filled circles) and ones without (represented by open circles). In static fatigue (Fig. 7(a)), cracks annealed without a preload subsequently grew slower by almost 1 order of magnitude. No such difference was found in cyclic fatigue at 1 Hz (Fig. 7(c)) and above and the retardation effect at 0.1 Hz (Fig. 7(b)) was also more moderate. In the following, the cause for such annealing effects based on knowledge of crack-tip mechanics will be speculated on.

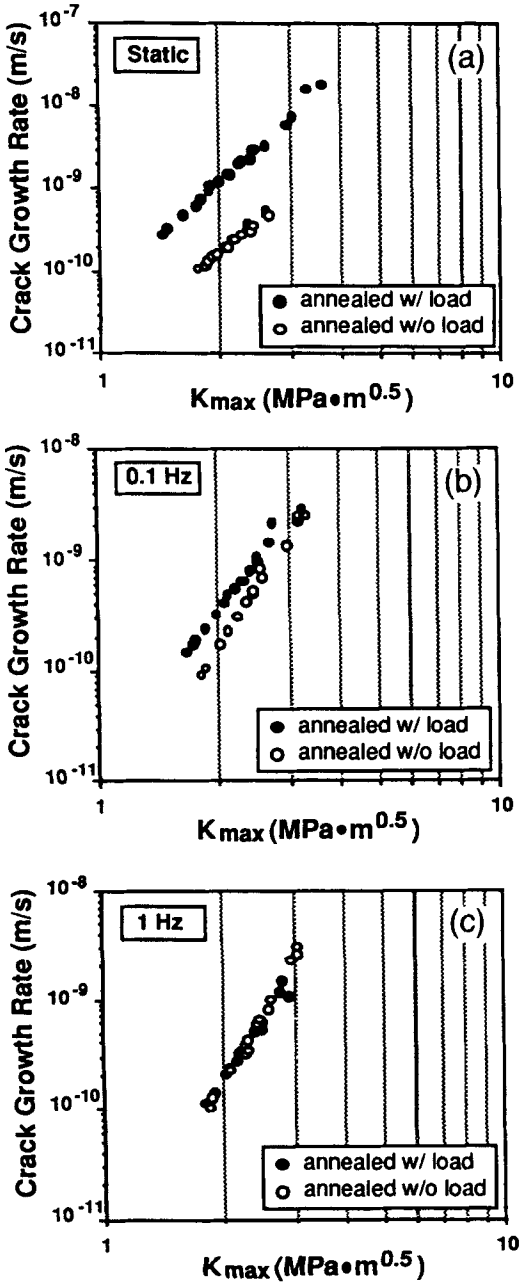

Fig. 7. Comparison of fatigue crack growth rates of specimens subject to different prior annealing treatment (a) static fatigue, and cyclic fatigue at (b) 0.1 Hz and (c) 1 Hz.

Assuming that, without a load applied, the annealing at 1400°C was able to blunt or heal the crack tip. In static fatigue, the crack face is not bridged by pulled-out grains. Hence, the effective stress intensity at the crack tip depends sensitively on the crack-tip geometry. A blunt or healed crack therefore experiences retardation until the crack tip is resharpened during subsequent loading. This could account for the behavior seen in Fig. 7(a). In high-frequency cyclic fatigue, on the other hand, the crack tip is subject to repeated damage which could develop a sharp crack tip at the same time of effecting extensive pullout. (Recall Fig. 6(a) for evidence.) In such a case (heavily bridged crack), the crack-tip geometry is of less importance in determining the stress intensity factor and, at any rate, a sharp crack tip could obtain soon after stress cycling. Therefore, the initial crack-tip geometry does not substantially influence the subsequent crack growth behavior. The frequency dependence of this pre-load/annealing effect is consistent with the above interpretation.

IV. Conclusions

(1) An effective test methodology by four-point bending with a short inner span and multiple controlled flaws was developed for the fatigue testing of structural ceramics at high temperatures.

(2) For a hot-pressed Si_3N_4 with 70 vol% (elongated) β-Si_3N_4 and 30 vol% (equiaxed) α'-sialon, the crack growth rate at 1400°C was slower under cyclic loading than under sustained loading, even after the effect of load-time profile was accounted for. This observation is consistent with the longer lifetime under cyclic loading which has been reported in the ceramic literature.

(3) The fatigue retardation effect was pronounced at higher frequency and lower stress intensity factor. Evidence for fatigue enhanced (β-Si_3N_4) grain pullout which could cause crack shielding and decreased crack growth rate was obtained.

(4) Annealing at 1400°C without load prior to fatigue testing greatly suppressed the subsequent crack growth rate in static fatigue, but not in cyclic fatigue (especially at higher frequencies). This implies that the crack-tip stress intensity of an unbridged crack, as in static fatigue, is highly sensitive to crack-tip geometry and blunting during high-temperature annealing. A similar blunting effect is apparently unimportant for a bridged crack as in cyclic fatigue at high temperature.

Acknowledgments: We are grateful to Dr. T.-S. Sheu for preparing the material and Dr. X. Wu for assistance during the initial stage of this research.

References

[1]S.-Y. Liu and I-W. Chen, "Fatigue of Yttria-Stabilized Zirconia: I, Fatigue Damage, Fracture Origins, and Lifetime Prediction," *J. Am. Ceram. Soc.*, **74** [6] 1197–205 (1991).

[2]S.-Y. Liu and I-W. Chen, "Fatigue of Yttria-Stabilized Zirconia: II, Crack Propagation, Fatigue Striations, and Short-Crack Behavior," *J. Am. Ceram. Soc.*, **74** [6] 1206–16 (1991).

[3]R. H. Dauskardt, D. B. Marshall, and R. O. Ritchie, "Cyclic Fatigue-Crack Propagation in Magnesia-Partially-Stabilized Zirconia Ceramics," *J. Am. Ceram. Soc.*, **73** [4] 893–903 (1990).

[4]R. H. Dauskardt, W. Yu, and R. O. Ritchie, "Fatigue Crack Propagation in Transformation-Toughened Zirconia Ceramic," *J. Am. Ceram. Soc.*, **70** [10] C-248–C-252 (1987).

[5]R. H. Dauskardt, D. B. Marshall, and R. O. Ritchie, "Cyclic Fatigue Crack Propagation in Ceramics: Behavior in Overaged and Partially Stabilized MgO-Zirconia"; pp. 543–50 in Proceedings of the Joint Symposium on Fracture Mechanics/Structural Mechanics, Materials Research Society International Meeting on Advanced Materials, Ikebukuro, Tokyo, Japan, June, 1988. Materials Research Society, Pittsburgh, PA, 1989.

[6]F. Guiu, M. J. Reese, and D. A. J. Vaughan, "Cyclic Fatigue of Ceramics," *J. Mater. Sci.*, **26**, 3275–86 (1991).

[7]F. Guiu, "Cyclic Fatigue of Polycrystalline Alumina in Direct Push–Pull," *J. Mater. Sci.*, **13,** 1357–61 (1978).

[8]M. J. Reece, F. Guiu, and M. F. R. Sammur, "Cyclic Fatigue Crack Propagation in Alumina under Direct Tension-Compression Loading," *J. Am. Ceram. Soc.*, **72** [2] 348–52 (1989).

[9]M. Reece and F. Guiu, "Repeated Indentation Method for Studying Cyclic Fatigue in Ceramics," *J. Am. Ceram. Soc.*, **73** [4] 1004–13 (1990).

[10]G. Grathwohl and T. Liu, "Crack Resistance and Fatigue of Transforming Ceramics: I, Materials in the ZrO_2–Y_2O_3–Al_2O_3 System," *J. Am. Ceram. Soc.*, **74** [2] 318–25 (1991).

[11]G. Grathwohl and T. Liu, "Crack Resistance and Fatigue of Transforming Ceramics: II, CeO_2-Stabilized Tetragonal ZrO_2," *J. Am. Ceram. Soc.*, **74** [12] 3028–34 (1991).

[12]J. F. Tsai, C. S. Yu, and D. K. Shetty, "Fatigue Crack Propagation in Ceria-Partially-Stabilized Zirconia (Ce-TZP)-Alumina Composites," *J. Am. Ceram. Soc.*, **73** [10] 2992–3001 (1990).

[13]S. Horibe, "Fatigue of Silicon Nitride Ceramics under Cyclic Loading," *J. Eur. Ceram. Soc.*, **6,** 89–95 (1990).

[14]D. S. Jacobs and I-W. Chen, "Environmental and Mechanical Contributions to Cyclic and Static Fatigue in Si_3N_4 and Al_2O_3"; presented at the 94th Annual Meeting of the American Ceramic Society, Minneapolis, MN, April 15, 1992 (Paper No. 2-JXI-92).

[15]D. A. Krohn and D. P. H. Hasselman, "Static and Cyclic Fatigue Behavior of a Polycrystalline Alumina," *J. Am. Ceram. Soc.*, **55** [4] 208–11 (1972).

[16]C. P. Chen and W. J. Knapp, "Fatigue Fracture of an Alumina Ceramic at Several Temperatures"; pp. 691–707 in *Fracture Mechanics of Ceramics 2.* Edited by R. C. Bradt, A. G. Evans, D. P. H. Hasselman, and F. F. Lange. Plenum Press, New York, 1973.

[17]B. K. Sarkar and T. G. J. Glinn, "Fatigue Behavior of High-Al_2O_3 Ceramics," *Trans. Br. Ceram. Soc.*, **69,** 199–203 (1970).

[18]M. V. Swain, "Lifetime Prediction of Ceramic Materials," *Mater. Forum*, **9,** 34–44 (1986).

[19]M. Masuda, N. Yamada, T. Soma, M. Matsui, and I. Oda, "Fatigue of Ceramics (Part 2)—Cyclic Fatigue Properties of Sintered Si_3N_4 at Room Temperature," *J. Ceram. Soc. Jpn.*, **97** [5] 520–24 (1989).

[20]M. Masuda, T. Soma, M. Matsui, and I. Oda, "Cyclic Fatigue of Sintered Si_3N_4," *Ceram. Eng. Sci. Proc.*, **9** [9–10] 1371–82 (1988).

[21]M. Masuda, T. Soma, and M. Matsui, "Cyclic Fatigue Behavior of Si_3N_4 Ceramics," *J. Eur. Ceram. Soc.*, **6,** 253–58 (1990).

[22]T. Kawakubo, N. Okabe, and T. Mori, "Static and Cyclic Fatigue Behavior in Ceramics"; pp. 717–26 in *Fatigue 90*, Proceedings of the Fourth International Conference on Fatigue and Fatigue Thresholds. Edited by H. Kitagawa and T. Tanaka. Materials and Component Engineering Publications Ltd., Birmingham, U.K., 1990.

[23]C.-K. J. Lin and D. F. Socie, "Static and Cyclic Fatigue of Alumina at High Temperatures," *J. Am. Ceram. Soc.*, **74** [7] 1511–18 (1991).

[24]T. Makino, Y. Nakasuji, M. Masuda, and M. Matsui, "Fatigue Behavior of Non-Oxide Ceramics under Static and Cyclic Stresses"; pp. 189–94 in Proceeding of the 1st International Symposium on the Science of Engineering Ceramics. Edited by S. Kimura and K. Niihara. Ceramic Society of Japan, Tokyo, Japan, 1991.

[25]M. Masuda, T. Makino, Y. Nakasuji, and M. Matsui, "Fatigue Behavior of Non-Oxide Ceramics at Elevated Temperature"; pp. 481–91 in *Fracture Mechanics of Ceramics*, Vol. 9. Edited by R. C. Bradt *et al.* Plenum Press, New York, 1992.

[26]T. Fett, G. Himsolt, and D. Munz, "Cyclic Fatigue of Hot-Pressed Si_3N_4 at High Temperatures," *Adv. Ceram. Mater.*, **1** [2] 179–84 (1986).

[27]M. Masuda, T. Soma, M. Matsui, and I. Oda, "Fatigue of Ceramics (Part 3): Cyclic Fatigue Behavior of Sintered Si_3N_4 at High Temperature," *J. Ceram. Soc. Jpn., Int. Ed.*, **97,** 601–607 (1989).

[28]L. X. Han and S. Suresh, "High-Temperature Failure of an Alumina–Silicon Carbide Composite under Cyclic Loads: Mechanisms of Fatigue Crack-Tip Damage," *J. Am. Ceram. Soc.*, **72** [7] 1233–38 (1989).

[29]S. Suresh, "Fatigue Crack Growth in Ceramic Materials at Ambient and Elevated Temperatures"; pp. 759–68 in *Fatigue 90*, Proceedings of the Fourth International Conference on Fatigue and Fatigue Thresholds. Edited by H. Kitagawa and T. Tanaka. Materials and Component Engineering Publications Ltd., Birmingham, U.K., 1990.

[30]S. Suresh, "Fatigue Crack Growth in Brittle Materials," *J. Hard Mater.*, **2** [1–2] 29–54 (1991).

[31]L. Ewart and S. Suresh, "Elevated-Temperature Crack Growth in Polycrystalline Alumina under Static and Cyclic Loads," *J. Mater. Sci.*, **27,** 5181–91 (1992).

[32]A. G. Evans and E. R. Fuller, "Crack Propagation in Ceramic Materials under Cyclic Loading Conditions," *Metall. Trans.*, **5A** [1] 27–33 (1974).

[33]A. G. Evans, L. R. Russel, and D. W. Richerson, "Slow Crack Growth in Ceramic Materials at Elevated Temperatures," *Metall. Trans.*, **6A** [4] 707–16 (1975).

[34]W. Blumenthal and A. G. Evans, "High Temperature Failure of Polycrystalline Alumina: II, Creep Crack Growth and Blunting," *J. Am. Ceram. Soc.*, **67** [11] 751–59 (1984).

[35]S. Buskovic, K. J. Lee, and T. Y. Tien, "Reaction Sintering of β-Si_3N_4/α′-SiAlON Ceramics"; pp. 373–80 in Materials Research Society Symposium Proceedings, Vol. 287, *Silicon Nitride Ceramics*. Edited by I-W. Chen, P. F. Becher, M. Mitomo, G. Petzow, and T.-S. Yen. Materials Research Society, Pittsburgh, PA, 1993.

[36]J. C. Newman, Jr., and I. S. Raju, "Analyses of Surface Crack in Finite Plates Under Tension or Bending Loads," NASA Technical Paper 1578 (available from National Technical Information Service, Springfield, VA), 1979.

[37]ASTM Standard E. 740-80, "Standard Recommended Practice for Fracture Testing with Surface-Crack Tension Specimens"; pp. 740–50 in *ASTM Annual Book of Standards*, Vol. 3.01. American Society of Testing and Materials, Philadelphia, PA, 1983.

[38]S.-Y. Liu and I-W. Chen, "Fatigue Deformation Mechanisms of Zirconia Ceramics," *J. Am. Ceram. Soc.*, **75** [5] 1191–204 (1992).

[39]I-W. Chen and A. S. Argon, "Grain Boundary and Interphase Boundary Sliding in Power Law Creep," *Acta Metall.*, **27,** 749–54 (1979).

[40]S.-Y. Liu and I-W. Chen, "High-Temperature Fatigue of Structural Ceramics"; presented at the 95th Annual Meeting of the American Ceramic Society, Cincinnati, OH, April 20, 1993 (Symposium on Fracture, Deformation, and Mechanical Reliability of Ceramics, Paper No. SIX-60-93). □